

# Optical Properties of Ferrofluids: Vorticity and Viscoelastic Measurements

J.-C. Bacri\* B. M. Heegaard, R. Perzynski

*Laboratoire d'Acoustique et Optique de la Matière Condensée<sup>†</sup>*

*Université Pierre et Marie Curie, Tour 13, Case 78 4 place Jussieu, 75252 Paris Cedex 05, France*

and

D. Zins

*Laboratoire de Physicochimie Inorganique URA CNRS SRSI*

*Université Pierre et Marie Curie, Bât. B, Case 63,*

*4 place Jussieu, 75252 Paris Cedex 05, France*

Received September 4, 1994

Magnetic particles are used as nanoscopic tools to probe locally the carrier in which they are suspended. In very dilute systems, the experimental detection of a field-induced optical birefringence allows to test liquid solutions, viscoelastic media and a liquid flow. Two examples are here developed: a study of the sol-gel transition of a chemical system and a vorticity measurement in a liquid sample experiencing a solid rotation.

## I. Introduction

If spectacular effects are observed with concentrated Magnetic Fluids (MF), with unexpected instabilities (starfishes)<sup>[1]</sup> or surprising properties (negative magnetic viscosity)<sup>[2]</sup>, very dilute magnetic fluids also deserve a growing interest. If a very small amount of magnetic particles is dispersed in a carrier medium, these nanoscopic objects can be used as rheological probes to investigate local properties of the medium. The strengths of such a method are that:

- the system is not perturbed by the nanoscopic tool, which occupies a volume fraction of the order of a few  $10^4$  (indeed this requires initial chemical work, to make the surface of magnetic particles fully compatible with the external medium)<sup>[3,4]</sup>.

- the magnetic field, used as an external parameter to monitor the movement of the particles, does not

perturb the carrier medium, if this one is an ordinary liquid, a polymer solution or a gel.

Standard magnetic measurements could not be easily performed with such a small amount of magnetic particles. We use here a well known property of particles, chemically synthesized using Massart's method<sup>[4]</sup>: they bear an intrinsic birefringence which allows a very accurate optical detection of their rotation. Different kinds of particle rotations can be induced with different kinds of exciting fields (static, pulsed, alternating, rotating). Here we shall only present some examples of what it is possible to probe with a static field and a pulsed one.

Depending on the carrier medium, birefringence response to a static magnetic field is ruled by a balance between different energies: in a simple liquid, it is a balance between magnetic and thermal energies; in a gel,

---

\*Affiliation: Université Paris 7

<sup>†</sup>Associated with the Centre National de la Recherche Scientifique

magnetic energy is compared to the elastic one. In the same order of ideas, by applying to an external static field to a flowing liquid, doped in magnetic particles, it is possible to measure a vorticity through a balance between the magnetic torque and the viscous one.

In each case, a pulsed magnetic field allows an analysis of the dynamical response of the system: in a simple liquid, for example, it is a test of the viscosity of the solution. Another quality of the present probing is the spatial scale of the measurement. In any viscometer, it is possible to define a length  $d$ , characteristic of the device, at which the viscosity measurement is performed (in a Couette viscometer,  $d$  is the distance between cylinders; in a capillary viscometer,  $d$  is the capillary diameter). In such usual viscometers, the viscosity measurement is always macroscopic:  $d \gg a$ ,  $a$  being a characteristic length of the probing system. In a single liquid,  $a$  is the size of the individual molecules (a few Å); in a gel,  $a$  is the mesh size of the polymeric array. In our system,  $d$  is the size of the magnetic particles, i.e. of the order of a few nanometers. We can either make a macroscopic measurement, either a mesoscopic one, either a microscopic one depending of the hierarchy between  $a$  and  $d$ . In a simple liquid, the measurement is macroscopic ( $d \gg a$ ). In a semi-dilute polymeric solution the measurement can be mesoscopic ( $d \simeq a$ ). In a very weak gel, it is possible to make a microscopic measurement ( $d \ll a$ ) using a very small perturbing magnetic energy: it allows studies close to a sol-gel transition.

If particles probe the carrier medium at their own spatial scale, an optical device performs the birefringence measurement through an average over the whole extension of the laser beam. Using well collimated beams, it is possible to map a sample in 2D or 3D:

-in a gel, inhomogeneities of elastic constants in a sample near a solid wall or a free surface can be explored.

-in a flowing liquid, vorticity maps can be also performed. We present now three examples of studies which can be performed with these nanoscopic probes.

## II. Birefringence properties in a magnetic liquid: Competition between Magnetic and Thermal Energies

It is well-known since more than 10 years that some magnetic fluid possess birefringent properties. In spite of controversy about the origin of this birefringence, a lot of applications are already possible<sup>[5-7]</sup>. This birefringence can come from a crystalline origin or a shape origin, but experimental measurements fit very well with theoretical laws including a log normal size distribution<sup>[8,9]</sup>; Except for a normalization factor, this theoretical law does not depend on the microscopic origin of this birefringence if measurements are concerned with individual behaviour. In some cases, chains of particles can be formed; under the applied field this effect is then tested through the shape of the experimental

We have verified that birefringence effects occur only if the particle turns mechanically and follows the magnetic field. It means that we need rigid-dipole particles with  $KV > k_B T$  where  $K$  is the anisotropic constant,  $V$  volume of the particle,  $k_B T$  thermal energy; in this case, the optical axis is parallel to the magnetic moment. The dielectric tensor is:

$$\epsilon_{ik} = n_0^2(\delta_{ik} + \gamma\phi S_{ik}), \quad (1)$$

where  $n_0$  is the isotropic index of the magnetic fluid at zero magnetic field,  $\gamma$  is the optic anisotropy of the particles,  $\phi$  its volume fraction and  $S_{ik}$  is a tensor describing the orientation ordering of optical anisotropy: without magnetic field,  $S_{ik} = 0$  and  $\epsilon_{ik} = n_0^2\delta_{ik}$ . If a field  $H = H\underline{h}$  ( $\underline{h}$  unit vector) is now applied, magnetization of the solution follows a Langevin law:  $\mathbf{M} = m_s\phi L(\xi)$  where  $\xi = \mu_0\mu H/kT$ . ( $\mu_0$  vacuum permeability,  $\mu$  mag-

netic moment of particles,  $L(\xi)$  is Langevin function:  $L(\xi) = \coth(\xi) - \xi^{-1}$  and  $m_s$  the particle magnetization. If  $\underline{h} = (1, 0, 0)$  is pointing in the same plane as the polarized light beam, birefringence  $\Delta n(H) \simeq (\epsilon_{xx} - \epsilon_{yy})/2n_0^2$  is obtained from a thermal average  $\langle e_j e_k \rangle_{th}$  of the microscopic tensor, introducing orientational distribution function  $W^0(\underline{e})$  of optical axes in Fokker-Planck equation<sup>[10]</sup>. At equilibrium it leads to:

$$\Delta n(H) = \delta n_s \phi S(\xi), \quad (2)$$

with

$$\delta n_s = \frac{3}{4} n_0 \gamma$$

and  $S(\xi) = 1 - 3L(\xi)/\xi$ . Such an expression fits well experimental measurements of static birefringence, providing that a size distribution of finite width is introduced in the treatment<sup>[8,9]</sup>.

The analysis of dynamical birefringence, as a response to a pulse of magnetic field, can be used to measure the viscosity of the liquid carrier. This powerful method working in a large range of viscosities ( $10^{-3}$  Paxs to  $10^4$  Paxs) is described in<sup>[11]</sup> and briefly recalled in next part for a simple colloid.

## II. Birefringence properties in a magnetic gel: Competition between Magnetic and Elastic Energy

The most important problem is to incorporate magnetic particles in the gel. Roughly speaking, two types of gel exist; chemical gels where the polymerization and the cross-link of monomers are irreversible with time and physical gels where the cross-links are reversible with temperature. With our method, we are able to study such transitions, called sol-gel transitions, usually well described by a percolation theory; for example the viscosity in the sol-phase increases in the vicinity of the transition with a critical exponent and the elastic constant in the gel phase vanishes critically.

This kind of experiments has been made some years ago in a physical gel (gelatin) and a critical exponent

has been measured<sup>[12]</sup>. We describe now the critical behaviour of a chemical gel<sup>[13]</sup>: an alumino-silicate in a mixture of water and isopropyl alcohol (*iPr* OH). The dynamical response to a pulse of magnetic field is analysed during the sol-gel transition<sup>[14]</sup>. For a given temperature, the control parameter is the time: following the preparation, the gel time can be monitored from an hour to a week. A very small amount of magnetic particles (volume fraction  $3 \times 10^{-4}$ ) is introduced in the initial sol phase in order to test the medium without perturbing it. In the sol phase, critical variation of the viscosity is obtained through a measurement of the characteristic time of birefringence relaxation at the field switching off. In the gel phase, the intensity of the birefringent signal and its relaxation time depend on elastic constant and friction coefficient. The experimental set-up used here is a standard ferrofluid viscometer device<sup>[11]</sup>. A pulse of magnetic field leads to a pulse of transmitted light intensity.

In a simple colloid such as the doped reagent and if the pulse length is long enough to reach a birefringence maximum, the relaxation of light intensity  $I(t)$  writes<sup>[11]</sup>:

$$I(t) = I_H \exp(-t/\tau_R) \quad (3)$$

with

$$I_H = I(t=0) \propto \Delta n(H)^2. \quad (4)$$

- The relaxation is a simple exponential, if the size distribution is thin enough;

- Origin of time,  $t = 0$  denotes the end of the magnetic pulse.

- The relaxation time  $\tau_R$  is  $\tau_R = \tau_B/\delta$ ,  $\tau_B$ : Brownian relaxation time,  $\tau_B = 3\eta V_h/kT$ ,  $\eta$ : carrier viscosity,  $V_h$ : hydrodynamic volume of particles,  $kT$ : thermal energy.

In a gel phase, there is a competition between magnetic and elastic energy<sup>[12]</sup>: the birefringence  $\Delta n(H)$  also depends on the local elastic constant. If we admit that all magnetic grains are blocked in the gel network and if  $\beta_0$  is the angle in zero field between H direction and the particle optical axis, the equilibrium angle  $\beta$ , in the limit  $x \ll 1$ , is given by:

$$u_0 \mu H \sin \beta = C V_c (\beta - \beta_0) , \quad (5)$$

where C is the local shear elastic constant and  $V_c$  the elastic perturbed volume. The value  $\Delta n(H, C)$  is given by a complex formula obtained after both a statistical average on  $\beta_0$  and a thermal average. The decay time is obtained from:

$$f V_c \beta' + C V_c (\beta - \beta_0) = 0 , \quad (6)$$

where  $f$  is the friction coefficient between the polymer network and the solvent leading to the characteristic time:

$$\tau_R \propto f / C . \quad (7)$$

In the sol-gel system, a simple exponential law does not fit correctly the experimental relaxation and has to be replaced by a stretched exponential one:

$$I(t) = I_H \exp(-t/\tau_R)^\alpha \quad (8)$$

characterized by a relaxation time  $\tau_R$ , the exponent accounting for the spatial inhomogeneities of the system<sup>[15]</sup> during the gelation process. Indeed  $\alpha$  is a function of  $\theta$ : the time spent from the initial blending to the moment of measurement, and  $\alpha(\theta = 0) = 1$ . Experimental times  $t$  and  $\tau_R$  are always small with respect to variations of  $\theta$ . Three kinds of plots are presented in figure 1:

- a linear plot of  $I(t)$  (figure 1a) leading to determinations of  $I_H = I(t = 0)$  and  $\tau_R$  from the condition  $I(t = \tau_R) = I_H/e$ ;

- a plot of  $\ln(I(t))$  as a function of  $t$  (figure 1b), to show that during the sol-gel process, a simple exponential fit cannot work;

- a log-log plot of  $-\ln(I(t)/I_H)$  as a function of  $t/\tau_R$  (figure 1c). In such a representation, experimental results exhibit a linear behaviour, expressing that they can be described by a stretched exponential relaxation, the slope of straight line being equal to the exponent  $\alpha$ .

In short, as a function of time  $\theta$ , three quantities are extracted from this stretched exponential treatment: initial intensity  $I_H$ , characteristic time  $\tau_R$  and exponent  $\alpha$ .

Preliminary results obtained with alumino-silicate system are presented in Figs. 2 and 3. It must be pointed out that  $\tau_R$  begins to increase drastically from its sol value far before  $I_H$  begins to decrease and that its divergence occurs during  $I_H$  decrease (cf fig. 2). Noteworthy variations of both  $I_H$  and  $\tau_R$  are thus shifted from each others. Another point is that  $\alpha$  varies all along the gelation process, from  $\alpha = 1$  at the beginning ( $\theta = 0$ ), through  $\alpha = 0.42$  at  $\tau_R$  divergence and blocks itself at a value  $\alpha = 0.3$  at the end of the experiment (see Fig. 3). Then, in a regime which is not explored here, a simple stretched exponential analysis cannot work anymore; the relaxation presents two co-existing and very distinct behaviours: a quick elastic answer and a long time relaxation.

During the gelation process, clusters more and more numerous are growing, leading to an increase of the mean viscosity of the system. In the experiment, this induces an increase of characteristic time  $\tau_R$  by more than three orders of magnitude and a decrease of exponent  $\alpha$  from its initial value 1, by more than a factor of two. At the gel point  $\theta_g$ , an infinite cluster is created and viscosity diverges: we may associate this to the  $\tau_R$  divergence.

The  $I_H$  decrease simply expresses that a larger and larger proportion of magnetic particles, trapped in large clusters, are not able to align completely along the field. After  $\tau_R$  divergence, if some free magnetic particles still remain in solvent pockets, they are less and less numerous with time and the dominant contribution becomes the elastic answer of the network which leads to a decrease of both  $I_H$  and  $r \sim$  .

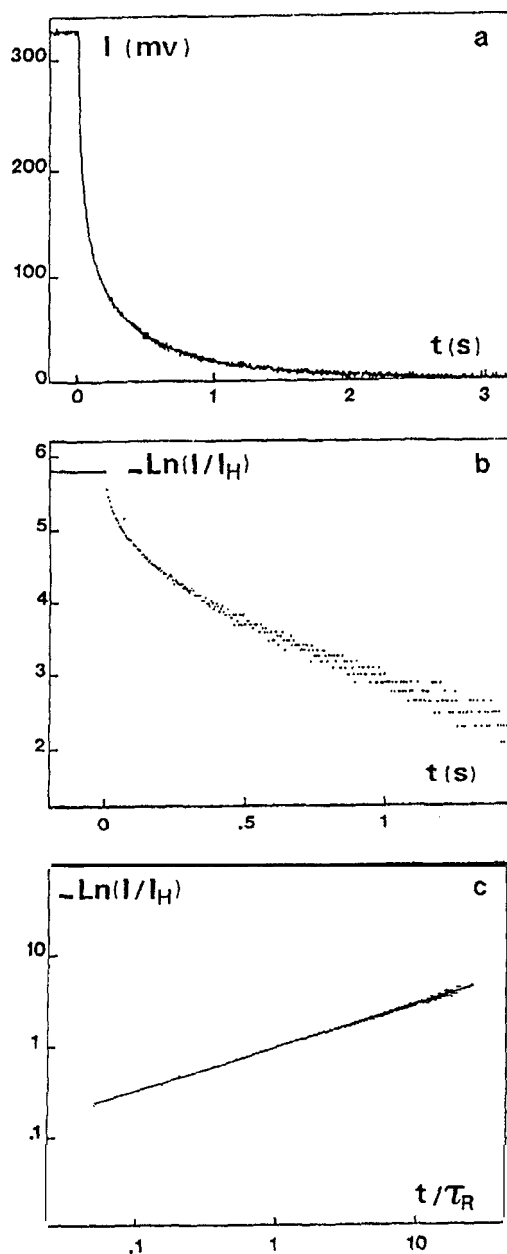


Figure 1: Relaxation measurements at  $\theta = 24h49'$ . (a) linear plot  $I(t)$ . (b) semi-log plot  $I(t)$ . (c) log-log plot of  $-\ln(I(t)/I_H)$  as a function of  $t/\tau_R$ . Straight line figures stretched exponential behaviour with  $I_H = 327$  mV,  $\tau_R = 100$  ms and  $\alpha = 0.48$ .

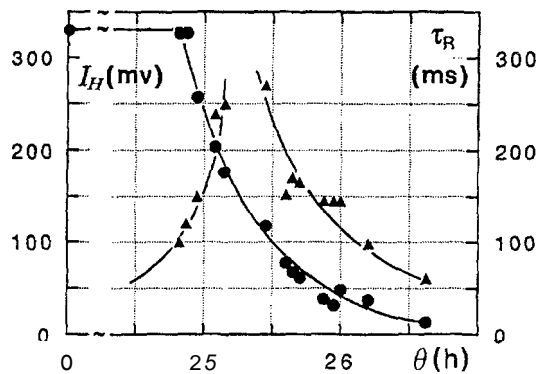


Figure 2: Double plot of  $I_H$  (black dots and left vertical axis) and  $\tau_R$  (triangles and right vertical axis) as a function of  $\theta$  near the gel point. Full lines are guides for the eye.

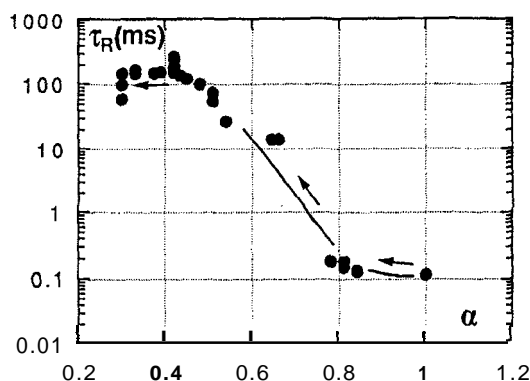


Figure 3: Semi-log plot of relaxation time  $\tau_R$  as a function of exponent  $\alpha$ .  $\theta$  is increasing from right to left. Full line is guide for the eye.

The greatest difficulty encountered in probing a highly non-homogeneous medium with the present experimental technique, was the strongly non-exponential dynamic response of the magnetic particles. During the gelation process, a stretched exponential relaxation correctly accounts for the dynamic magnetic birefringence. In Ref. [15], a similar behaviour is observed with electric birefringence relaxation in systems as different as critical binary mixtures, polydisperse micellar solutions and dilute polyelectrolyte solutions. The  $\alpha$  exponent, related to local inhomogeneities of the system is a quantity which is, exactly as the characteristic time  $\tau_R$ , modified far before the gel point (see fig. 3). This implies that during the sol-gel process, while the mean viscosity increases, the system at the local scale of our magnetic probes, becomes more and more inhomogeneous with largely polydispersed clusters. In

the present study, magnetic particles are randomly oriented inside the clusters. A relaxation experiment under a large external magnetic field<sup>[16]</sup> could allow to analyse the dynamic of large clusters with trapped-in magnetic particles all aligned together.

### III. Magnetic fluid in a flow: Competition between Magnetic and Hydrodynamic Torque

If physicists want to increase their experimental knowledge in order to explain the route to the turbulence, they need a powerful tool for vorticity measurements at a local scale. A small amount of magnetic particles in a liquid does not perturb the flow even with a magnetic field. The idea of the vorticity measurement is to measure locally the orientation of the optical axis of the solution which reflects the balance between the hydrodynamic and the magnetic torques experienced by the particles in a constant magnetic field in the flow.

We present here preliminary results<sup>[17]</sup> with a system of constant vorticity in a rotating sample in a constant magnetic field perpendicular to the vorticity.

If in the formalism of part I, a vorticity  $\underline{\Omega} = (0, 0, \Omega)$  is added, thermodynamical equilibrium is disturbed by the flow, reading the new orientational distribution function  $W(\underline{e})$  as an expansion around  $W^0(\underline{e})$ , steady state solution of Fokker-Planck Eq. [10], to first order in  $\Omega\tau_{\perp}$ , leads to:

$$S_{ik} = \begin{bmatrix} S(\xi) & \frac{2}{3}\Omega\tau_{\perp}S(\xi) & 0 \\ \frac{2}{3}\Omega\tau_{\perp}S(\xi) & -\frac{1}{2}S(\xi) & 0 \\ 0 & 0 & \frac{1}{2}S(\xi) \end{bmatrix}, \quad (1)$$

with  $\tau_{\perp} = \tau_B \frac{2L(\xi)}{\xi - L(\xi)}$ . The tensor  $S_{ik}$  is symmetric and can be diagonalized through a rotation of angle  $\rho$  in plane  $(x, y)$ . This angle  $\rho$  between external field and solution optical axis is:  $\rho = \Omega\tau_{\perp}$ . As field intensity is increased, birefringence  $\Delta n(H)$  increases:  $S(\xi)$  is growing from zero to unity for  $\xi \rightarrow \infty$ . On the contrary,  $\rho$  decreases, as the relaxation time  $\tau_{\perp}$  which lowers from  $\tau_B$  in the limit  $\xi \rightarrow 0$  to zero for  $\xi \rightarrow \infty$ , where  $\tau_{\perp}$  behaves as  $\tau_H = 2\tau_B/\xi$ . An experimental measurement of  $\rho$  will allow a determination of  $\Omega$ .

To the third order in  $\Omega\tau_{\perp}$ , previous calculations<sup>[18]</sup> lead to:

$$\tan(\rho) = \Omega\tau_{\perp} (1 - ((8 + 3\xi L(\xi))/(2 + \xi, L(\xi)))(\Omega\tau_{\perp})^2). \quad (2)$$

The ferrofluid sample is put between two glass plates (cell thickness:  $e = 110\mu\text{m}$ ), rotating at angular velocity  $\Omega$ . A linearly polarized laser beam of low power 1mW ( $\lambda = 0.63\mu\text{m}$ ), goes along the axis of rotation, through the sample. An analyser is glued on the rotating cell. A static external magnetic field  $\underline{H}$ , parallel to the beam polarization and perpendicular to  $\underline{\Omega}$ , embeds the ferrofluid (see fig 4). Neglecting the sample dichroism, the light intensity collected by the photodiode is:

$$I = I_t(\cos^2(\Omega t) + \cos^2(\Omega t - 2\rho) + \cos\Psi[\cos^2(\Omega t) - \cos^2(\Omega t - 2\rho)]), \quad (3)$$

with  $\Psi = 2\pi e\Delta n(H)/\lambda$ . The detected intensity is a periodic function of time, of pulsation  $2\Omega$ : in zero field, it is equal to  $I_0 = I_t(1 + \cos 2\Omega t)$ . The signal is then analysed with a lock-in amplifier. We measure experimentally the phase shift  $\phi = 2\Omega t_{\min}$  of a minimum of  $I$  as a function of field intensity  $H$ . Minimizing  $I$  with

respect to  $t$ , leads to:

$$\tan(\phi) = \sin^2(\Psi/2)\sin 4\rho / (\cos^2(\Psi/2) + \sin^2(\Psi/2)\cos 4\rho) \quad (4)$$

where both  $\rho$  (cf expression (9)) and  $\Psi = 2\pi e\delta n_s \Phi S(\xi)/\lambda$  are field dependent.

The ferrofluid samples used here are dilute colloids ( $\Phi \approx 2\%$ ) of nanometric magnetic particles in suspension in glycerol ( $\eta = 1 \text{ Pa.s}$ ). The particles are chem-

ically synthesized through Massart's method<sup>[4]</sup>, coated with citrate ligands<sup>[3]</sup>, and are made of Cobalt ferrite<sup>[9]</sup> ( $S_n = 8 \times 10^{-2}$ ).

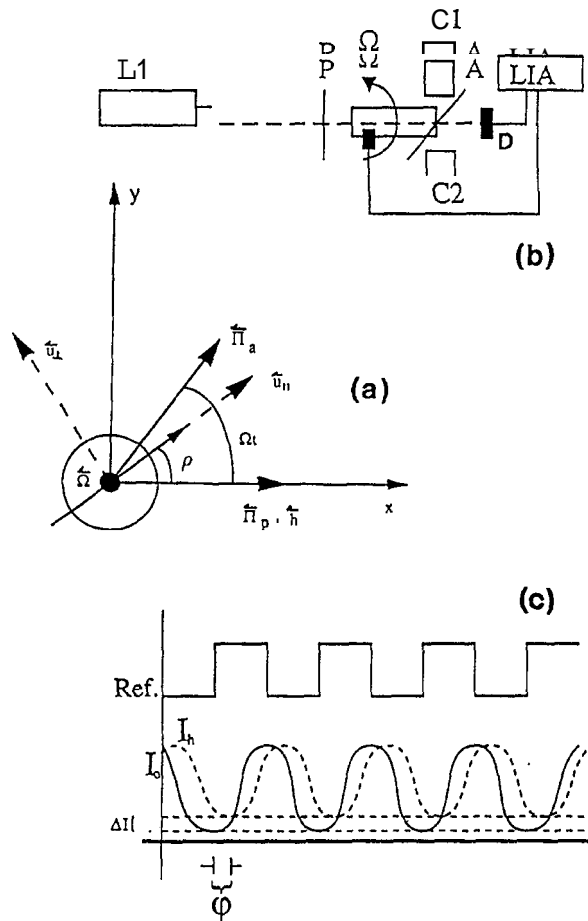


Figure 4: (4a) Map in the sample plane ( $Q_x, Q_y$ ) of unit vectors, respectively pointing in direction of: polarizer ( $\hat{\Pi}_p$ , magnetic field ( $\hat{h}$ , analyser ( $\hat{\Pi}_A$ ) rotating with angular velocity  $\Omega$ , sample optical axis ( $\hat{E}_s$ ), ( $\hat{E} \sim \hat{I}(\hat{E}_s)$ ), and  $\rho$  angle between ( $\hat{h}$ ) and ( $\hat{u}_p$ ). (4b) Experimental set-up:  $L_1$  He-Ne laser;  $P$  polarizer;  $\Omega$  angular velocity of the sample cell;  $C_1$  and  $C_2$  are polepieces of electromagnet providing us with magnetic field perpendicular to ( $\hat{\Omega}$ );  $A$  analyser glued on sample;  $D$  photodiode; LIA lock-in amplifier to detect the phase-lag. (4c) Schema of temporal dependence of detected intensity:  $\rho$  is the field dependent phase shift of the minimum intensity.

Fig. 5 presents variations of measured phase shift  $\varphi$  as a function of applied field  $H$  for the three angular velocities, 160, 190 and 220 rad/s. Full lines on Fig. 5 are theoretical plots of a size distribution averaged quantity:  $\langle \varphi_{sda} \rangle = \int_0^\infty \varphi P(d) dd$ , taking into account the particle dispersity with a log-normal distribution  $P(d)$  of diameters  $d$ ,  $d_{mp}$  being the most probable diameter

and  $\sigma$  the standard deviation.  $\varphi$  is given by expressions (1) and (2) in which volume fraction then writes  $\phi(d) = \Phi d^3 / \langle d^3 \rangle$ . The best fits are realized taking  $\tau_B$  as an independent parameter and lead to:  $\tau_B = 3$  ms,  $d_{mp} = 13$  nm, and  $\sigma = 0.4$ . The model developed in the theoretical part accounts correctly for the measurements ( $\Omega\tau_B = 0.6$  means  $\Omega\tau_B < 1$ ),  $\tau_B$  determination leads to an hydrodynamic diameters  $d_h = 20$  nm compatible with  $d_{mp}$  value.

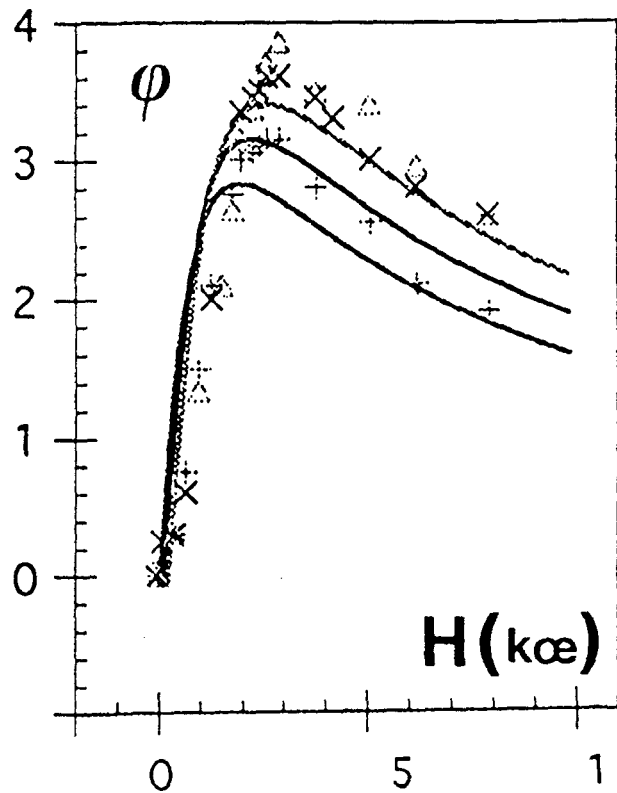


Figure 5: Experimental phase shift  $\varphi$  (in degrees) as a function of magnetic field  $H$  for different angular velocity: from bottom to top, 160 (+), 190 (x) and 220 rad  $s^{-1}$  (A). The continuous lines are theoretical fits  $\langle \varphi_{sda}(H) \rangle$  using parameters  $d_{mp} = 13$  nm,  $u = 0.4$ , and  $\tau = 3$  ms.

With such a sample of volume fraction of particles of the order of 2%, the maximum phase shift is of the order of 3 degrees (to first order proportional to  $\Omega\tau_B$ ). To use this technique at lower  $\Omega\tau_B$  values, one will have to adjust both particle concentration and detection sensitivity. In the future we will extend this experiment to ordinary flows and to vorticity maps in 2D or 3D.

Through the few examples developed here, the power of this simple optical method is obvious. Future applications of this nanoscopic tool will be the lo-

cal probing of viscoelastic media such as gels or liquid crystals and vorticity measurements in more complicated flows.

## References

1. J.-C. Bacri, A. Cebers and R. Perzynski, submitted to Phys. Rev. Lett..
2. M. Shliomis and K. Morozov, submitted to Physics of Fluids A.
3. J.-C. Bacri, R. Perzynski, D. Salin, V. Cabuil and R. Massart, J. Mag. Mat. 85, 27 (1990).
4. R. Massart, Patent: France 7918842, 9006484; Germany P3027012.3; Japan 98.202/80; U.S.A. 4329241.
5. H. Davies and P. Llewellyn, J. Phys. D. 12, 1357 (1979).
6. S. Taketomi, H. Takahashi, N. Inaha, H. Miyajima and S. Chikazumi, J. Phys. Soc. Japan 59, 2500 (1990).
7. J.-C. Bacri and R. Perzynski, in *Complex Fluids* Lecture Notes in Physics (Springer Verlag, Berlin, 1992) p. 415.
8. J.-C. Bacri, V. Cabuil, R. Massart, R. Perzynski and D. Salin, J. Mag. Mat. 65, 285 (1987).
9. S. Neveu, F.A. Tourinho, J.-C. Bacri and R. Perzynski, Colloids and Surfaces A 80, 1 (1993).
10. M. A. Martsenyuk, YU. L. Raikher and M. Shliomis, Proc. of Int. Conf. Magn. (I.C.M.-73), Moscow, Nauka 3, 540 (1974).
11. J.-C. Bacri, J. Dumas, D. Gorse, R. Perzynski and D. Salin, J. Physique Lett. (France) 46, L- 1 199 ( 1985).
12. J.-C. Bacri and D. Gorse, J. Physique (France) 44, 985 (1983).
13. F. Chaput, J.-P. Boilot, F. Devreux, M. Canva, P. Georges and A. Brun, Symp. Proc. Materials Research Society 271, 663 (1992).
14. J.-C. Bacri, J.-C. Boilot, R. Massart, L. Malier, R. Perzynski and D. Zins, Proc. of the Internat. Symp. on Aerospace and Fluid Science, Sendai, Japan, (1993) p. 680.
15. V. Degiorgio, R. Piazza, F. Mantegazza and T. Bellini, J. Phys.: Cond. Matter 2, SA.69 (1990).
16. J.-C. Bacri, K. Djerfi, S. Neveu and R. Perzynski, J. Mag. Mat. 123, 67 (1993).
17. J.-C. Bacri, B. M. Heegaard, S. Neveu, R. Perzynski and M. Shliomis, Proc. of the Internat. Symp. on Aerospace and Fluid Science, Sendai, Japan, (1993) p. 643.
18. J.-C. Bacri, B. M. Heegaard, R. Perzynski and M. Shliomis, Journées de l'hydrodynamique de la montagne Sainte Geneviève, EN.S., Paris, France, April 1993 (to be published)